JOURNAL OF Materials CHEMISTRY

Changes of the lamellar period by nanoparticles in the nanoreactor scheme of thin films of symmetric diblock copolymers

Byeongk-Hyeok Sohn,* Byung-Wook Seo and Seong-Il Yoo

Department of Materials Science and Engineering, Polymer Research Institute, Pohang University of Science and Technology, Pohang 790-784, Korea. E-mail: bhsohn@postech.ac.kr

Received 18th February 2002, Accepted 28th March 2002
First published as an Advance Article on the web 2nd May 2002

Nanometre-sized domains of block copolymers can be utilized as so-called nanoreactors to synthesize a variety of nanoparticles. In this nanoreactor scheme, the domain size and period of block copolymers should be expanded to incorporate nanoparticles. We investigated changes in the domain period by gold nanoparticles, employing thin films of symmetric polystyrene-*block*-poly(4-vinylpyridine) (PS–PVP) diblock copolymers. Since the PS–PVP thin film on the substrate had a multilayered structure of parallel lamellae with a film thickness quantized in terms of the lamellar period, thickness measurements after *in situ* synthesis of gold nanoparticles in the PVP lamellae enabled us to quantify changes in the lamellar period. In addition, we measured the amount of gold nanoparticles incorporated into the film using a quartz crystal microbalance. From these results, dependence of the lamellar period on the volume fraction of nanoparticles can be explained by an intermediate case of homogeneous distribution and local segregation of nanoparticles within the PVP lamellae.

1. Introduction

Nanoparticles of metal, semiconductor, and oxide are of great interest because they are expected to have novel electrical, optical, magnetic, and catalytic applications.[1] Nanometre-sized domains of block copolymers can be utilized as so-called nanoreactors to synthesize such nanoparticles.[2–14] That is, block copolymers self-assemble into a variety of periodic structures on the tens of nanometre length scale[15] and nanoparticles can be selectively synthesized *in situ* within the self-assembled domains. For example, we recently synthesized gold nanoparticles selectively in the lamellar domains of diblock copolymers to fabricate a multilayered nanostructure of alternating pure polymeric lamellae and gold nanoparticle-containing lamellae.[14]

In the nanoreactor scheme based on *in situ* synthesis of nanoparticles, the domain size and period of block copolymers should be expanded to incorporate nanoparticles within the domains. In addition, amounts of nanoparticles incorporated without altering the domain structure could be limited. To investigate changes in the domain period, especially in a lamellar morphology, we employed thin films of symmetric diblock copolymers, which can be easily fabricated by spin coating with a controlled thickness. We were able to quantify changes in the lamellar period from thickness measurements because the thin film had a multilayered structure of lamellae parallel to the film plane with a quantized thickness in terms of the lamellar period.[15–22]

For unconfined films of symmetric diblock copolymers on the substrate, the relative interfacial energies between each block and the substrate, and the relative surface energy of each block induce a preferential wetting of one block at an interface.[15–22] Consequently, the lamellar structure is oriented parallel to the film plane. Due to commensurability effects of film thickness with a lamellar period (L_o), the film thickness should be quantized in values of nL_o for symmetric wetting, *i.e.* the same block at both interfaces, and $(n + 1/2)L_o$ for asymmetric wetting, *i.e.* one block at the free surface and the other at the substrate interface. If the initial film thickness is not commensurate with this constraint, terraces (islands or holes) form on the free surface of the film with a step height of L_o to maintain the natural period of lamellae. Therefore, we can accurately evaluate the lamellar period and its change induced by nanoparticles from the film thickness and the terrace height, which can be conveniently measured by atomic force microscopy (AFM).[22]

In this study, we investigated changes of the lamellar period by gold nanoparticles synthesized *in situ* in thin films of symmetric polystyrene-*block*-poly(4-vinylpyridine) (PS–PVP) diblock copolymers. The thin film had a multilayered nanostructure consisting of alternating polymer layers and gold nanoparticle layers, which has potential applications in electronics and photonics, including one dimensional photonic bandgap materials due to periodic repeats of the refractive index of each layer.[23]

2. Experimental

2.1. Diblock copolymers

Polystyrene-*block*-poly(4-vinylpyridine) (PS–PVP) was purchased from Polymer Source Inc. The number average molecular weights of PS and PVP were 21 400 g mol^{-1} and 20 700 g mol^{-1}, respectively. The polydispersity index was 1.13. The glass transition temperature measured by DSC (5 °C min^{-1}) was 102 °C for the PS block and 138 °C for the PVP block. The lamellar period before synthesis of gold nanoparticles (L_o), evaluated from AFM measurements, was 28 nm.

2.2. Substrates

Silicon wafers were cleaned in a piranha solution (70/30 *v*/*v* of concentrated H_2SO_4 and 30% H_2O_2) at 90 °C for 20 min, and thoroughly rinsed with deionized water several times, and then blown dry with nitrogen. Fresh mica substrates were prepared by cleaving a piece of mica. Both substrates after cleaning or cleaving were immediately used for the spin coating of copolymers.

 DOI: 10.1039/b201752k

2.3. Thin films of diblock copolymers

Thin PS–PVP films were spin-coated onto clean silicon wafers or freshly cleaved mica from an *N*,*N*-dimethylformamide (DMF) solution. A film with a thickness of 78 nm ($2.8L_o$) or 92 nm ($3.3L_o$) was obtained by adjusting spinning speed and solution concentration. The copolymer film was annealed at 180 °C in a vacuum oven for 36 h.

2.4. Synthesis of gold nanoparticles

We employed a relatively well-developed method to synthesize gold nanoparticles from $HAuCl_4$ as a precursor and $NaBH_4$ as a reducing reagent.[5,6,9–11,14] The PS–PVP thin film was immersed into 1 wt% ethanol solutions of $HAuCl_4$ for about 30 min, then thoroughly rinsed with deionized water several times. To obtain an equilibrium loading of the precursor, a dipping period of the film in the solution was selected when the film weight was not increased further by a quartz crystal microbalance. The thin film loaded with $HAuCl_4$ was again dipped into 1 wt% $NaBH_4$ solutions for about 30 s to reduce the precursors to gold nanoparticles. Longer dipping of the film in the reduction solution did not affect gold nanoparticle formation but damaged the film. The same cycle of loading of precursors and reducing to gold nanoparticles was repeated to increase the volume fraction of gold nanoparticles in the film. After each cycle, the film was rinsed with deionized water several times and was completely dried at 60 °C in a vacuum oven for longer than 24 h to avoid swelling by water.

2.5. Transmission electron microscopy (TEM)

With PS–PVP thin films containing gold nanoparticles, cross-sectional TEM samples were prepared as described in the literature.[14] From the thin film embedded in epoxy with carbon coating on both sides of the film after removing the substrate, thin sections (*ca.* 70 nm thick) were obtained using a Reichert Ultra Microtome with a diamond knife. TEM was performed on a JEOL 1200EX at 120 kV and a JEOL 2010F at 200 kV in high resolution.

2.6. Atomic force microscopy (AFM)

Surface topography of thin films was imaged using AFM (AutoProbe CP Research, Park Scientific Instruments) in contact mode. After scraping away some of the film from the substrate with a razor blade, the film thickness was measured from several different areas to obtain an average value. The height of terraces (islands or holes) was similarly obtained. From the film thickness and the terrace height, we evaluated the lamellar period of the thin film before and after the synthesis of gold nanoparticles.

2.7. Quartz crystal microbalance

The weight of the thin film after each synthesis cycle of gold nanoparticles was measured by a quartz crystal microbalance (QCM, EG&G-Seiko Model 917).[24] A gold-plated quartz crystal was used as a working electrode. Thin films of diblock copolymers were spin-coated and annealed on mica substrates and were peeled off from the mica substrate by immersing them in water. Then, a floated film was collected onto the gold electrode plated on a quartz crystal, and annealed above the glass transition temperatures of both blocks of the copolymers for shorter than 24 h to secure the film on the electrode. After measuring an initial weight of the film from a frequency shift, synthesis of gold nanoparticles was directly performed with the film on the electrode and an increase of the film weight was measured.

3. Results and discussion

A PS–PVP thin film with a thickness of 78 nm ($2.8L_o$) or 92 nm ($3.3L_o$) was spin-coated and annealed far above the glass transition temperatures of both blocks on silicon wafers or mica substrates. Since the PS block has a lower surface energy and the PVP block has a preferential interaction with silicon wafers or mica substrates, multilayered lamellae parallel to the substrate were induced with an asymmetric wetting configuration, *i.e.* the PVP block at the substrate interface and the PS block at the air interface. The film thickness before annealing ($2.8L_o$ or $3.3L_o$) was not commensurate with $(n + 1/2)L_o$. Thus, after annealing, a $2.8L_o$-thick film had a quantized thickness of $2.5L_o$ with islands in a step height of L_o. Similarly, in a $3.3L_o$-thick film, the thickness was quantized as $3.5L_o$ with holes in a step height of L_o, as shown in Fig. 1. The substrate exposed by scraping away the film to measure a total film thickness appeared on the right part of the AFM image in Fig. 1. In the height profile, the total film thickness should be equal to the quantized thickness of $3.5L_o$. Also, the depth of holes corresponding to gray areas in the image should have a value of L_o. From the film thickness and the hole depth, the lamellar period before gold nanoparticle synthesis (L_o) was measured as 28 nm. We obtained the same value of L_o with the film having the quantized thickness of $2.5L_o$ with islands. We also evaluated the lamellar period after nanoparticle synthesis using both thin films having holes and islands.

We synthesized gold nanoparticles selectively into the PVP layer of PS–PVP thin films having holes or islands as demonstrated in our previous study.[14] Thin PS–PVP films were immersed in ethanol solutions of $HAuCl_4$ until the film weight was not increased further. A $HAuCl_4$ molecule can be coordinated to a pyridine unit of the PVP block by protonation. Estimated from a 127% increase of the film weight on treatment

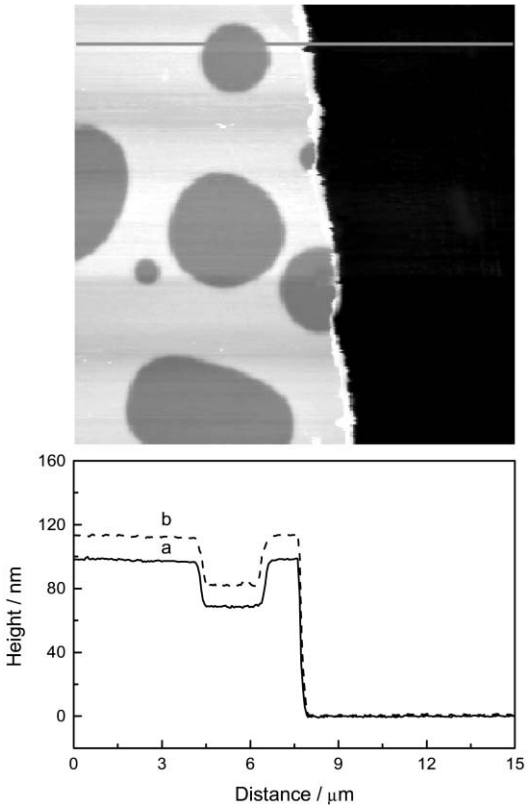

Fig. 1 AFM image of a PS–PVP thin film quantized in a $3.5L_o$ thickness with holes in a step height of L_o on the film. The dark area on the right part corresponds to the substrate exposed by scraping away the film. Holes in the film appear as gray areas. Along the line in the image, height profiles (a) before and (b) after 4 synthesis cycles of gold nanoparticles are given below the image.

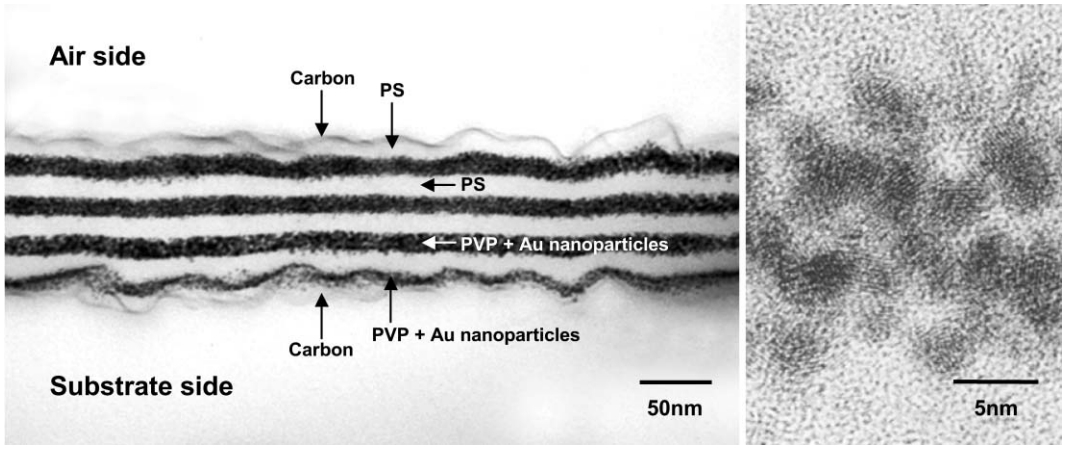

Fig. 2 Cross-sectional TEM image of a PS–PVP thin film containing gold nanoparticles. The film had a quantized thickness of $3.5L_o$. A high-resolution image of gold nanoparticles in the thin film is shown on the right side.

with $HAuCl_4$, *ca.* 80% of the pyridine units of the PVP blocks was quaternized with $HAuCl_4$. Then, the selectively-loaded precursors were reduced to gold nanoparticles within the PVP layers by aqueous $NaBH_4$ solution. After reduction, the film weight was decreased, presumably due to removal of by-products and some of gold nanoparticles during the cleaning process. But the film weight after reduction was 110% larger than that before the loading and reducing cycle.

Fig. 2 shows a cross-sectional TEM image of the PS–PVP film after gold nanoparticle synthesis. Since the thin film was embedded in epoxy with carbon coating after removal of the substrate, the images were slightly undulated. The image clearly shows the multilayered structure of alternating PS layers and gold nanoparticle-containing PVP layers. The film had 3.5 PS layers and 3.5 nanoparticle-containing PVP layers, *i.e.* a quantized thickness of 3.5 lamellar periods with an asymmetric wetting configuration, *i.e.* the PS block at the air interface and the nanoparticle-containing PVP block at the substrate interface, indicated by arrows in the TEM image. Moreover, we can confirm that the synthesis of gold nanoparticles was performed homogeneously through the thin film, but selectively on the PVP lamellar layers without a diffusion problem of reagents.[14] Gold nanoparticles in each PVP layer appeared dense because the image of gold nanoparticles corresponds to the projection of all nanoparticles in a *ca.* 70 nm-thick microtomed slice. The size of gold nanoparticles was *ca.* 3 nm in diameter in the high-resolution image, as shown in the right side of Fig. 2. This film containing gold nanoparticles showed an absorption maximum around 540 nm in the UV–Vis spectrum. The result was similar to typical spectra observed in gold nanoparticles,[11] implying that effects of the layered structure on the optical property of gold nanoparticles were apparently inconsequential in this experimental condition.

After the first synthesis cycle of gold nanoparticles in PS–PVP thin films, the thickness and the hole depth were increased. The increase was ascribed to gold nanoparticles synthesized selectively in the PVP layers of the film, as confirmed in the TEM image of Fig. 2. In addition, the synthesis of gold nanoparticles did not alter the surface morphology of the film. The shape of holes or islands was maintained after the synthesis. Changes in hole or island diameters by the synthesis were also negligible. Therefore, the *in situ* synthesis of gold nanoparticles did not affect the multilayered structure of PS–PVP thin films so that the lamellar period after the synthesis of gold nanoparticles (L) was again evaluated from the total thickness and the height of holes or islands of the film containing gold nanoparticles. In addition, we repeated the synthesis cycle of gold nanoparticles with the same PS–PVP thin film. We were able to keep loading the precursor on to the film after each synthesis cycle, presumably due to regeneration of the coordination sites for $HAuCl_4$ in the PVP block after each cycle. However, the amount of $HAuCl_4$ loaded was decreased after each synthesis. Repeating the synthesis cycle did not alter the surface morphology of the film, although the surface became more or less rough after the synthesis cycle. Thus, the lamellar period after each cycle was again evaluated from the total thickness and the height of holes or islands. The height profile after 4 cycles of gold nanoparticle synthesis is shown in Fig. 1. It was almost impossible to quantify changes in the lamellar period from cross-sectional TEM images.

Fig. 3 shows the lamellar period of a PS–PVP thin film as a function of the number of cycles of gold nanoparticle synthesis. The lamellar period after each synthesis cycle (L) was normalized by the initial value before the nanoparticle synthesis (L_o). In addition, film weights (W) normalized by the initial film weight (W_o) after each cycle are shown in Fig. 4. As we can see, the lamellar period and the film weight were similarly increased by repeating the synthesis cycle. However, both values reached saturation after 4 synthesis cycles, presumably because the space available for gold nanoparticles in the PVP blocks was limited. To calculate the volume fraction of gold nanoparticles in the film from the weight increases in Fig. 4, we assumed that gold nanoparticles incorporated only affect the weight increase of the film, although some by-products of the synthesis could remain in the film even after washing the film. The density of

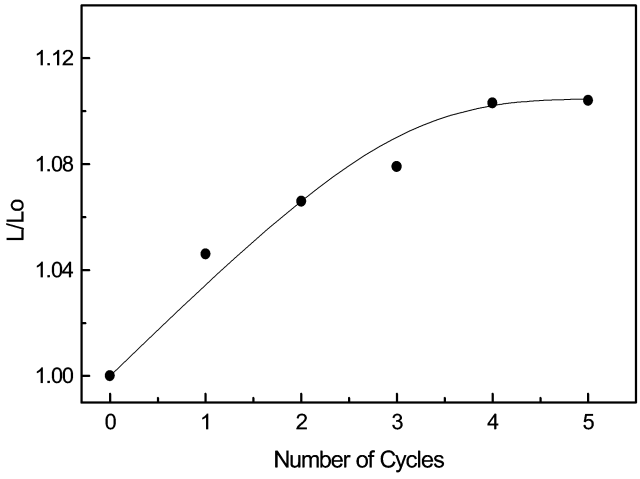

Fig. 3 Lamellar period of a PS–PVP thin film as a function of the number of synthesis cycles of gold nanoparticles. The lamellar period after each synthesis cycle (L) was normalized to the initial value before the nanoparticle synthesis (L_o).

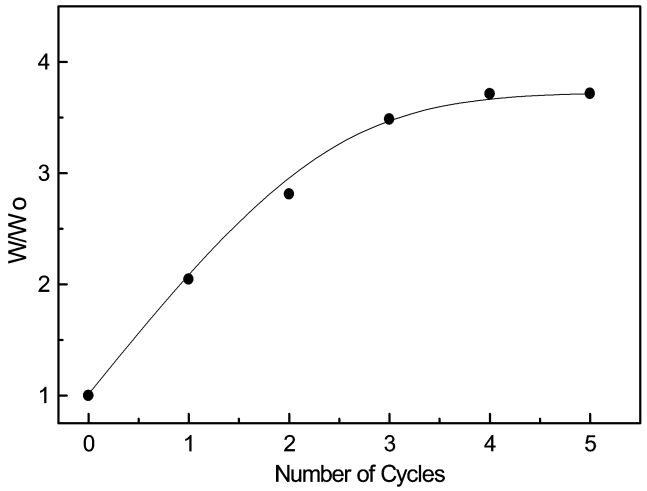

Fig. 4 Weight of a PS–PVP thin film as a function of the number of synthesis cycles of gold nanoparticles. The film weight after each synthesis cycle (W) was normalized to the initial value before the nanoparticle synthesis (W_o).

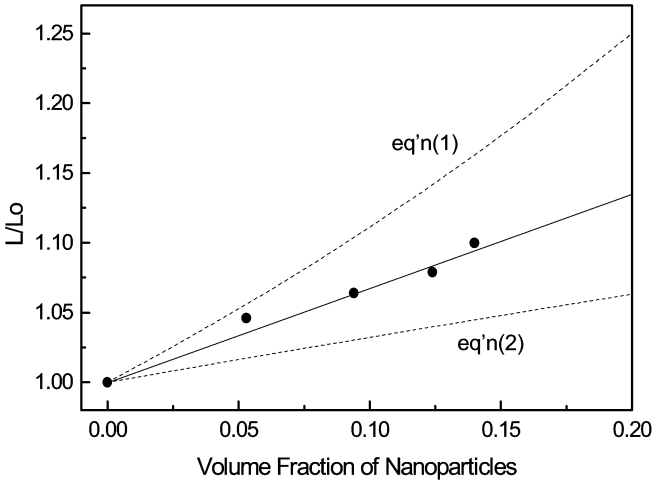

Fig. 5 Lamellar period of a PS–PVP thin film as a function of the volume fraction of gold nanoparticles. Curves calculated by eqn. (1) and (2) are also plotted for comparison.

gold nanoparticles was also assumed the same as the bulk value of gold.

Dependence of the lamellar period of a PS–PVP film on the volume fraction of gold nanoparticles is shown in Fig. 5. Although the maximum ratio of W/W_o after 4 repeats of the synthesis cycle was *ca.* 3.70 in Fig. 4, the corresponding volume fraction of gold nanoparticles was only about 0.14 due to the density of gold. The lamellar period showed a linear dependence on the volume fraction of gold nanoparticles. After each repeat of the synthesis cycle, not only the population but also the diameter of gold nanoparticles in the film could be increased. However it was very difficult to evaluate increases in the population and the diameter of gold nanoparticles from cross-sectional TEM images, largely because the density of gold nanoparticles in the image was too high even after the first repeat of the synthesis cycle due to the projected image of all nanoparticles in a microtomed slice. To compare with theoretical results,[25,26] we assume that every repeat of the synthesis cycle mainly increases the population of gold nanoparticles in the film with a narrow size distribution.

In a blend of A–B symmetric diblock copolymers with nanoparticles having interactions with the A block, nanoparticles can be dissolved in the A lamellar domains.[25] If nanoparticles are confined to the middle of the domains, a change of the lamellar period (L) can be expressed by

$$L/L_o = 1/(1 - \phi_{NP}) \quad (1)$$

where ϕ_{NP} is the volume fraction of nanoparticles in the film. This case is similar to blending of A–B symmetric diblock copolymers with A homopolymers that have a higher molecular weight than the A block.[22] Contrarily, in the case that nanoparticles are uniformly dissolved in the A lamellar domain, dependence of the lamellar period on the volume fraction of nanoparticles is

$$L/L_o = g(\phi_A, \phi_{NP})^{-1/3}/(1 - \phi_{NP}) \quad (2)$$

$$g(\phi_A, \phi_{NP}) = [\phi_A + (1 - \phi_A)\phi_{NP}^2]/\phi_A (1 - \phi_{NP})^2$$

where ϕ_A is the volume fraction of the A block of copolymers, which is 1/2 for symmetric diblock copolymers. The case of uniformly distributed nanoparticles in the domains is analogous to blending of A–B symmetric diblock copolymers with A homopolymers that have a lower molecular weight than the A block.[22] In the case of uniform distribution, intermingling of nanoparticles (or homopolymer chains) with chains of the A block resulted in the increase of the A lamellar thickness. However, by lateral swelling of the A lamellae, the B lamellae should be shrunk to maintain uniform density throughout the film. Since the thickness increase of the A lamellae was generally greater than the thickness decrease of B lamellae, the lamellar period was increased by the blending of nanoparticles (or homopolymers). Thus, an increase of the lamellar period by uniformly distributed nanoparticles is smaller than that by localized nanoparticles, as predicted by eqn. (1) and (2).

In Fig. 5, both lines calculated by eqn. (1) and (2) are included. As we can see, dependence of the lamellar period on the volume fraction of nanoparticles in this study did not follow either of the predicted lines, but lay between the two cases of localized and uniformly distributed nanoparticles. Since the precursor $HAuCl_4$ molecules were loaded into the film by protonation of pyridine units of the PVP block, the precursors should be homogeneously distributed in the PVP lamellae. Thus, gold nanoparticles after *in situ* reduction of the precursors could have more chances to locate between the PVP chains (uniform distribution) than between the ends of the PVP chains (local segregation in the middle of the domain). The lateral swelling of the PVP chains to accommodate nanoparticles could necessitate shrinkage of the covalently connected PS chains in order to maintain uniform density.[22,25,26] However, since we employed *in situ* synthesis of gold nanoparticles at room temperature instead of blending them with the copolymers, shrinking of the glassy PS chains could be limited. In addition, the lateral swelling of chains could be limited further in the thin film secured on the substrate. Thus, some of the particles could exist between the ends of the PVP chains, *i.e.* in the middle of the PVP lamellae. Thus, the lamellar period showed more increases than that in the case of uniform distribution of nanoparticles. Therefore, the nanoparticle distribution in this study can be explained as an intermediate case of homogenous distribution and local segregation of nanoparticles within the lamellae. However, it was not possible to distinguish between uniform distribution and local segregation of gold nanoparticles in the PVP lamellae from the cross-sectional TEM images (*e.g.* Fig. 2). Forward recoil spectroscopy[27] and Rutherford backscattering spectroscopy[28] were used to analyze particle distribution in polymer films. Secondary ion mass spectroscopy[17] and X-ray reflection standing wave fluorescence spectroscopy[29] could be other possible methods for probing nanoparticle distribution in thin films.

4.Conclusions

To investigate expansion of the nanometre-sized domains of block copolymers by nanoparticles synthesized *in situ*, a thin film of PS–PVP symmetric diblock copolymers was employed as an example of a nanoreactor. Since the thin film had a multilayered structure of lamellae parallel to the film plane with a quantized thickness in terms of the lamellar period, changes in the lamellar period were quantitatively evaluated from thickness measurements by AFM. Combining this result with the amount of gold nanoparticles in the film measured by a quartz crystal microbalance, the lamellar period showed intermediate increases by inclusion of gold nanoparticles, compared with the cases of homogeneous distribution and local segregation of nanoparticles within the lamellae.

Acknowledgement

This work was supported by the Korea Science and Engineering Foundation (Grant No.2000-2-30100-010-3). Facility support from the Center for Integrated Molecular Systems is gratefully acknowledged.

References

1 J. H. Fendler, *Nanoparticles and Nanostructured Films*, Wiley-VCH, Weinheim, Germany, 1998.
2 Y. Ng Cheong Chan, R. R. Schrock and R. E. Cohen, *Chem. Mater.*, 1992, **4**, 24.
3 B. H. Sohn and R. E. Cohen, *Chem. Mater.*, 1997, **9**, 264.
4 R. Saito, S. Okamura and K. Ishizu, *Polymer*, 1992, **33**, 1099.
5 J. P. Spatz, A. Roescher, S. Sheiko, G. Krausch and M. Möller, *Adv. Mater.*, 1995, **7**, 731.
6 J. P. Spatz, A. Roescher and M. Möller, *Adv. Mater.*, 1996, **8**, 337.
7 M. Moffitt, L. McMahon, V. Pessel and A. Eisenberg, *Chem. Mater.*, 1995, **7**, 1185.
8 B. Hamdoun, D. Ausserré, S. Joly, Y. Gallot, V. Cabuil and C. Clinard, *J. Phys. II*, 1996, **6**, 493.
9 A. B. R. Mayer and J. E. Mark, *Colloid Polym. Sci.*, 1997, **275**, 333.
10 M. V. Seregina, L. M. Bronstein, O. A. Platonova, D. M. Chernyshov, P. M. Valetsky, J. Hartmann, E. Wenz and M. Antonietti, *Chem. Mater.*, 1997, **9**, 923.
11 L. Bronstein, M. Antonietti and P. Valetsky, in *Nanoparticles and Nanostructured Films*, ed. J. H. Fendler, Wiley-VCH, Weinheim, Germany, 1998.
12 T. Hashimoto, M. Harada and N. Sakamoto, *Macromolecules*, 1999, **32**, 6867.
13 H. Mattoussi, L. H. Radzilowski, B. O. Dabbousi, D. E. Fogg, R. R. Schrock, E. L. Thomas, M. F. Rubner and M. G. Bawendi, *J. Appl. Phys.*, 1999, **86**, 4390.
14 B. H. Sohn and B. H. Seo, *Chem. Mater.*, 2001, **13**, 1752.
15 I. W. Hamley, *The Physics of Block Copolymers*, Oxford University Press, NewYork, 1998.
16 G. Krausch, *Mater. Sci. Eng.*, 1995, **R14**, 1.
17 G. Coulon, T. P. Russell, V. R. Deline and P. F. Green, *Macromolecules*, 1989, **22**, 2581.
18 T. P. Russell, G. Coulon, V. R. Deline and D. C. Miller, *Macromolecules*, 1989, **22**, 4600.
19 S. H. Anastasiadis, T. P. Russell, S. K. Satija and C. F. Majkrzak, *Phys. Rev. Lett.*, 1989, **62**, 1852.
20 M. D. Foster, M. Sikka, N. Singh, F. S. Bates, S. K. Satija and C. F. Majkrzak, *J. Chem. Phys.*, 1992, **96**, 8605.
21 J. Heier, E. J. Kramer, S. Walheim and G. Krausch, *Macromolecules*, 1997, **30**, 6610.
22 K. A. Orso and P. F. Green, *Macromolecules*, 1999, **32**, 1087.
23 Y. Fink, A. M. Urbas, M. G. Bawendi, J. D. Joannopoulos and E. L. Thomas, *J. Lightwave Technol.*, 1999, **17**, 1963.
24 M. D. Ward, in *Physical Electrochemistry*, ed. I. Rubinstein, Marcel Dekker, New York, 1995.
25 B. Hamdoun, D. Ausserré, V. Cabuil and S. Joly, *J. Phys. II*, 1996, **6**, 503.
26 J. Huh, V. V. Ginzburg and A. C. Balazs, *Macromolecules*, 2000, **33**, 8085.
27 K. R. Shull, K. I. Winey, E. L Thomas and E. J. Kramer, *Macromolecules*, 1991, **24**, 2748.
28 M. S. Kunz, K. R. Shull and A. J. Kellock, *J. Colloid Interface Sci.*, 1993, **156**, 240.
29 B. Lin, T. L. Morkved, M. Meron, Z. Huang, P. J. Viccaro, H. M. Jaeger, S. M. Williams and M. L. Schlossman, *J. Appl. Phys.*, 1999, **85**, 3180.